

Fully integrated dual-polarization silicon photonic transceiver with automated polarization control

Xinru Wu, Duanni Huang, Taehwan Kim, Ranjeet Kumar, Guan-Lin Su, Chaoxuan Ma, Songtao Liu, Ganesh Balamurugan, Haisheng Rong

Intel Corporation, 2200 Mission College Blvd, Santa Clara, CA 95054

Abstract: We demonstrate a dual-polarization, single-wavelength transceiver with BER below soft-decision FEC ($<2.0e-2$) at 320Gb/s (PAM-4) aggregate rate. The silicon photonic chip includes integrated laser, ring modulators, Si/Ge detectors, and polarization demux with automatic polarization control.

1. Introduction

Increasing the bandwidth per fiber is a critical requirement to meet rapidly increasing data traffic demands. For direct detection systems, the primary avenues to meet this bandwidth demand are increasing the Baud-rate (>100 GBaud), using higher-order modulation formats (PAM-4,8), increasing the number of wavelengths, and utilizing orthogonal polarizations of light. While dual-polarization (DP) transmission is a staple in coherent links, it is less frequently utilized in direct detection, due to the difficulty in demultiplexing the two polarizations at the receiver after random polarization change in the fiber. One demonstrated technique involves measuring the Stokes vector, which requires DSP to demux the polarizations in the electrical domain [1]. Recent work on optical polarization demux has been limited to the manual operation of polarization controllers [2], applicable to coherent links only [3,4], or does not enable DP [5]. In this work, we implement a marker-tone assisted polarization stabilization scheme that can automatically detect and track polarization changes in the fiber. We experimentally validate the scheme by transmitting 80GBaud PAM-4 data on each polarization with BER $<2.0e-2$ while the fiber undergoes polarization rotation at 0.02π rad/s. All devices on the transmitter and receiver are integrated and fabricated with Intel's 300nm silicon photonics process.

2. System Architecture

The schematic for the dual-polarization transmitter and receiver is shown below in Fig. 1. On the transmitter (TX) side, a hybrid silicon/III-V DFB laser at 1310nm with >13 dBm of output power is equally split between two waveguides. Two independent PAM-4 data streams modulate microring modulators in the two waveguides. After modulation, the polarization on the bottom arm is rotated from TE to TM, and light in the two waveguides is combined using a polarization splitter rotator (PSR). One of the arms includes a heater, which is used to dither the phase for that specific polarization to generate a marker tone. This enables efficient polarization demultiplexing at the receiver as explained later. The receiver (RX) chip uses a PSR to separate the incoming light into two waveguides, both with TE polarization. In general, the polarization state has been changed in the fiber, and arrives with an unknown state at the receiver. To recover the polarization state at the transmitter, the two arms are sent into a Mach-Zehnder interferometer (MZI) with phase tuners before and inside the interferometer. This structure serves as a dynamic polarization controller (DPC) [3]. By tuning the two heaters in the DPC, it is possible to realize any unitary matrix transfer function. Thus, the DPC can produce a transfer matrix that inverts the Jones matrix of the fiber to undo polarization rotation and birefringence effects in the fiber, assuming the polarization dependent loss (PDL) is negligible.

Since the marker tone is applied purely to the *phase* of signal on one TX polarization, it has no effect on the detected RX intensities when there is no mixing between the two polarizations. On the other hand, when the two polarizations are not exactly demultiplexed, beat tones at the marker tone frequency (and higher harmonics) will be detected by the PDs. Additionally, in the absence of PDL, equal power should be detected by the two PDs (Fig. 1). These two properties can be used to tune the DPC to achieve optimal demultiplexing by continuously adjusting the heaters in the DPC.

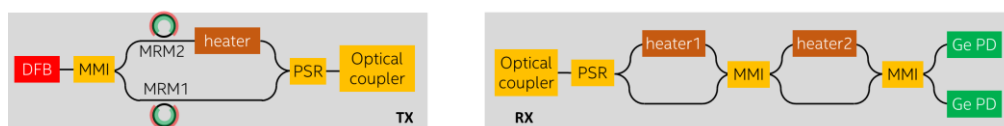


Fig 1. Schematic of the devices in the dual-polarization system.

3. Experimental Setup and Results

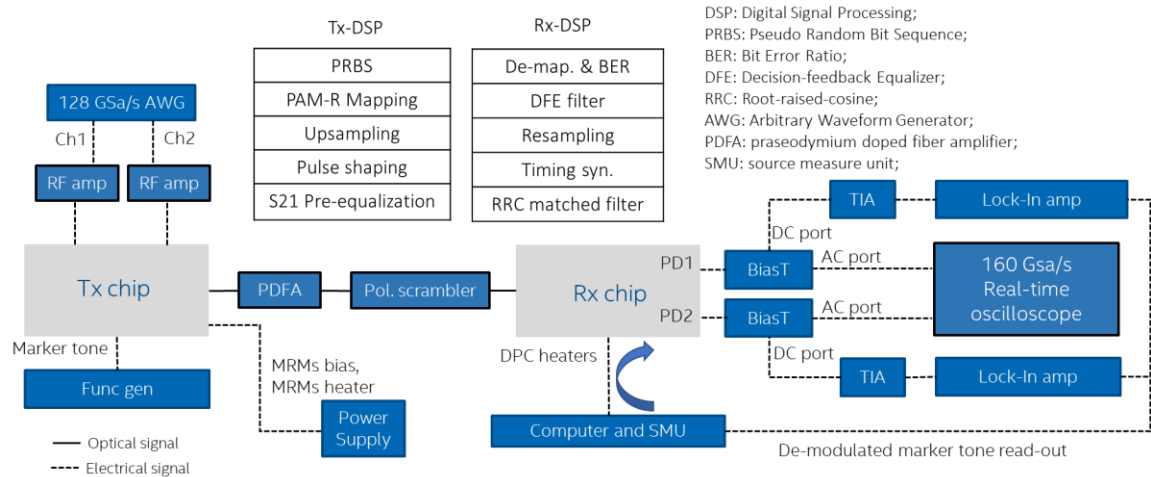


Fig 2. Diagram of experimental setup.

The experimental setup is shown above in Fig. 2. Two channels of an arbitrary waveform generator provide independent PAM-4 data streams at 80GBaud to the two microring modulators (MRMs), which have a 3dB OE bandwidth (BW) of 50GHz. An external function generator provides a small sinusoidal marker tone with $f = 3.3\text{kHz}$. A polarization scrambler is placed in between the TX and RX, as well as PDFA to compensate for coupling losses. A pair of bias-T are used at the RX PDs (BW $\sim 40\text{GHz}$) to provide bias for PDs as well as separate the low-speed marker tone from the high-speed PAM-4 data. The marker tone on each PD is then demodulated using a lock-in amplifier at If and $2f$, and the readings are summed on a lab computer along with the differential photocurrent of the two PDs after they are amplified through a transimpedance amplifier (TIA). The computer performs a gradient descent control algorithm to minimize the marker tone + differential photocurrent, and then feeds back new heater setpoints to the RX chip. Meanwhile, the high-speed data is simultaneously collected using two channels of a 160 Gsa/s real-time scope and processed offline to count bit errors. At the transmitter DSP, the 80GBaud PAM-4 signal is first up-sampled by a factor of 1.6 (128/80), followed by an RRC filter with a roll-off factor of 0.12 designated for pulse shaping. Pre-emphasis is implemented by using an inverted linear filter based on the channel frequency response. At the receiver side, a matched RC filter is performed to mitigate the effects of white noise. The received signal is re-sampled and then equalized with a (21,5)-tap decision-feedback equalizer.

To demonstrate the real-time polarization control and tracking, two experiments are performed. First, we initialize the system with an unknown Rx polarization state and random heater settings and turn on the control algorithm to converge to a demux condition. This is illustrated in Fig. 3. Prior to the experiment, a 2-D scan of the DPC heater settings is performed and the marker tone ($If + 2f$) plus differential photocurrent is recorded. This 2-D map is not needed for the algorithm to work but shown here to help illustrate the convergence to the demux condition. The 2-D map in Fig. 3(b) is periodic, with clear minima, which correspond to valid demux conditions. The initial heater setpoint is shown as a black star, which is far away from a demux condition. This is apparent from the large marker tone reading, as well as measured BER and eye diagram in Fig. 3(c). After the algorithm is initialized, the heaters are adjusted to decrease the marker tone, and a subsequent improvement in BER is observed after a few algorithm iterations. Eventually, the algorithm converges to a demux condition, which is the red triangle in Fig. 3(b), with BER reading $< 1e-2$ for both channels. In this experiment, the convergence process takes ~ 4 seconds, which is limited by the relatively long iteration time ($\sim 300\text{ms}$) due to instrument communication in the setup. The iterations can be much faster with dedicated FPGA hardware running gradient descent.

In the first experiment, the polarization scrambler is not engaged. The input polarization state is stable, and the heaters cease to move after the demux condition is reached. For the second experiment, we engage the polarization scrambler (Luna PSY-201) with a triangular scrambling trace at a rate of 0.02π rad/s. The system is initialized near the demux condition, and the control algorithm works to keep the system stabilized throughout the polarization scrambling. The results are shown in Fig. 4. For the first 45 seconds, the control algorithm is on, and the heaters are adjusted continuously on each iteration to track the polarization drift induced by the polarization scrambler. After 45 seconds, the algorithm is purposely turned off to illustrate the rapid walk-off in BER over just a few seconds. The measured BER is well below $2.0e-2$ for the duration of the tracking.

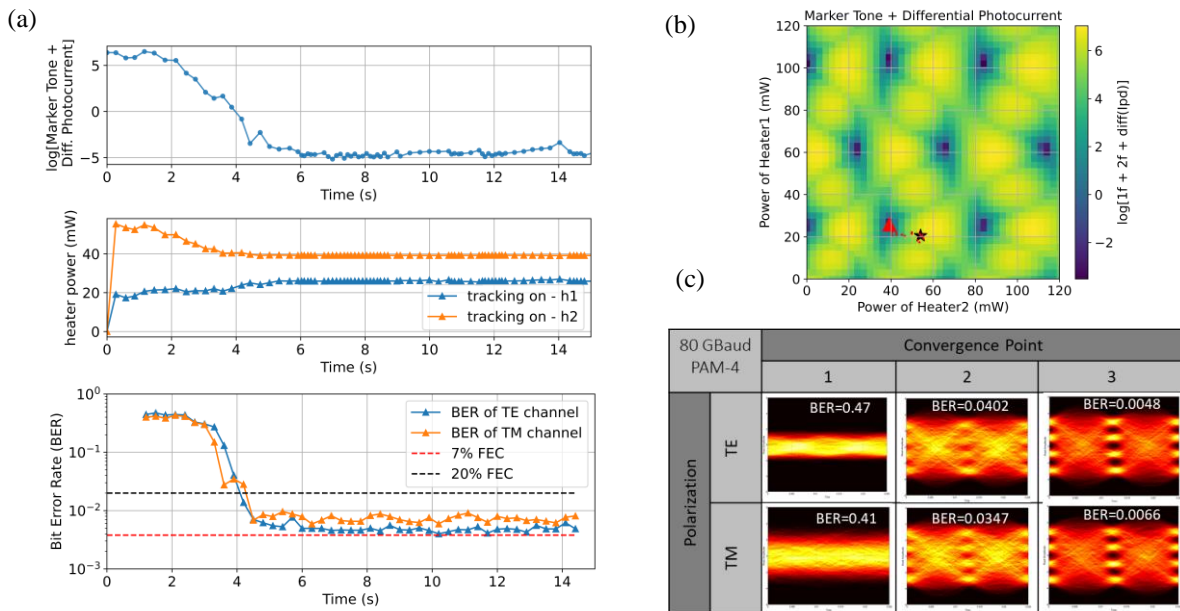


Fig. 3: (a) The detected marker tone + differential photocurrent, heater settings, and BER as the system converges to a demux condition. (b) The 2-D map of the $(1f+2f)$ marker tone plus differential photocurrent versus heater powers. The start and endpoints of the convergence algorithm are marked. (c) The eye diagrams when the system is (1) away, (2) nearby, (3) and fully converged to the demux condition.

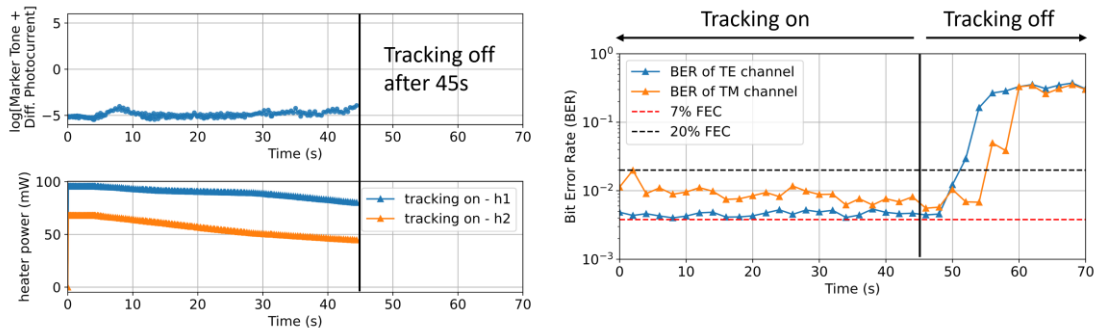


Fig. 4: The marker tone, heater settings, and BER as the system undergoes polarization rotation. The tracking is halted after 45 seconds, at which point the BER rapidly reaches unacceptable values.

4. Conclusion

We have demonstrated 320 Gbps transmission on a single wavelength using polarization multiplexing in an IM-DD link. The system impresses a phase marker tone on one polarization that is detected at the receiver to assist polarization demultiplexing. The polarization tracking is automated using a gradient descent algorithm and demonstrated in real-time to converge the system to the correct demux condition and stabilize it with $\text{BER} < 2.0 \times 10^{-2}$.

Acknowledgments

The authors would like to thank Bryan Casper, Meer Sakib, Peicheng Liao, Hasitha Jayatilika, and Panagiotis Zarkos for early contributions, James Jaussi, Yuliya Akulova, Saeed Fathololoumi, and Ling Liao for technical support and discussions, as well as our process engineers in F11X for device fabrication.

References

- [1] D. Che and W. Shieh, "Polarization demultiplexing for Stokes vector direct detection," *J. Light. Technol.* **34**(2), 754-760 (2016)
- [2] P. Liao, et al., "A 260 Gb/s/ λ PDM Link with Silicon Photonic Dual-Polarization Transmitter and Polarization Demultiplexer," *ECOC (2021)*
- [3] C. Doerr, et al., "PDM-DQPSK silicon receiver with integrated monitor and minimum number of controls," *IEEE Photon. Technol. Lett.* **24**(8), 697-699 (2012)
- [4] J. K. Perin, et al., "Design of low-power DSP-free coherent receivers for data center links," *J. Light. Technol.* **35**(21), 4650-4662 (2017)
- [5] M. Ma, et al., "Automated adaptation and stabilization of a tunable WDM polarization-independent receiver on active silicon photonic platform," *IEEE Photon. J.* **12**(4), 1-11 (2020)